OMICS Journal of Radiology

Case Report   **Open Access**

The Nose Knows: Imaging of Sinonasal Lesions

Akm A Rahman[1]*, Usman M Syed[2] and Steve J Stephen[2]

[1]Department of Imaging Sciences, University of Rochester Medical Center, USA
[2]School of Medicine and Dentistry, University of Rochester, USA

Abstract

Sinonasal tumors are more often malignant and comprise approximately 3% of all head and neck malignancies. Half of these tumors arise in the nasal cavity, and other common locations of origin include the ethmoid and maxillary sinuses. Some unique clinical features are anosmia and altered phonation but the most common general features include headache, epistaxis, and diplopia. CT and MRI may be used to assess tumor location, invasion of adjacent tissue, presence of metastasis, internal tumor heterogeneity, and contrast enhancement. Local invasion of the tumor beyond the sinonasal tract can impact adjacent structures such as the cranial nerves, skull base, branches of the internal carotid artery, and orbit leading to neurologic signs, facial pain, and diplopia. Imaging may be used to differentiate sinonasal tumors and predict the tumor subtype to aid in diagnosis, staging, and treatment planning. This collection of benign and malignant sinonasal tumors will include some rare and unique cases with an emphasis on imaging features demonstrating a wide variety of pathologies.

Keywords: Sinonasal Lesions; Squamous Cell Carcinoma; Adenoid Cystic Carcinoma; Sinonasal Undifferentiated Carcinoma; Esthesioneuroblastoma; Melanoma; Lymphoma; Rhabdomyosarcoma; Inverted Papilloma; Antrochoanal Polyp; Mucous Retention Cyst

Abbreviation

ACC – Adenoid Cystic Carcinoma; **ADC** – Apparent Diffusion Coefficient; **AP** – Antrochoanal Polyp; **AJCC** – American Joint Committee on Cancer; **C** – Contrast; **CT** – Computed Tomography; **DLBCL** – Diffuse Large B-Cell Lymphoma; **DWI** – Diffusion Weighted Imaging; **ENB** – Esthesioneuroblastoma; **FESS** – Functional Endoscopic Surgery; **IP** – Inverted Papilloma; **ITAC** – Intestinal Type Adenocarcinoma; **MRC** – Mucous Retention Cyst; **MRI** – Magnetic Resonance Imaging; **NHL** – Non-Hodgkin Lymphoma; **NKTL** – Natural Killer/T-Cell Lymphoma **RMS** – Rhabdomyosarcoma; **SCC** – Squamous Cell Carcinoma; **SNUC** – Sinonasal Undifferentiated Carcinoma **T1WI** – T1-weighted magnetic resonance imaging; **T2WI** – T2-weighted magnetic resonance imaging; **TNM** – Tumor, Node, Metastasis

Introduction

Sinonasal tumors are more commonly malignant than benign, more likely to present later in the disease course, and more often associated with poor prognosis [1]. Sinonasal malignancy is rare with an incidence rate of 0.56 per 100,000, a male:female ratio of 1.8:1, and a 3% proportion of all head and neck malignancies. The most common anatomical sites for sinonasal lesions include the nasal cavity (43.9%), the maxillary sinus (35.9%), and other paranasal sinuses [2]. Histologically, most malignant sinonasal tumors are classified as squamous cell carcinoma (51.6%) and other classification groups include adenocarcinoma (12.6%), sarcoma, melanoma, lymphoma, and sinonasal undifferentiated carcinoma (SNUC) [1,2] Imaging is an important aspect of the diagnosis, staging, and longitudinal assessment of sinonasal tumors [1].

Many sinonasal tumor types exhibit differentiating imaging features on CT and MRI such as anatomical location, invasion of adjacent tissue, metastasis, tumor homogeneity, internal signal intensity, and contrast enhancement. Additionally, apparent diffusion coefficient (ADC) mapping from diffusion weighted MR imaging (DWI) can assist with differentiating malignant from benign lesions, particular types of malignancy, and the tumor stage. Razek et al. reported significantly lower (p=0.001) ADC values for malignant lesions ($1.10 \pm 0.25 \times 10{-3}$ mm2/s) relative to benign lesions ($1.78 \pm 0.41 \times 10{-3}$ mm2/s) [3]. These imaging characteristics can be used to predict histological tumor subtype, evaluate pre-treatment prognosis, guide the choice of treatment modality, and determine tumor stage [1].

Overview of Sinonasal Tract Anatomy

The sinonasal tract consists of the nasal cavity and paranasal sinuses. The nasal cavity contains a midline nasal septum and 3-4 bilateral bone conchae with underlying meatuses to drain the paranasal sinuses. The paranasal sinuses are lined with respiratory epithelium and are extensions of the nasal cavity consisting of four bilaterally paired sinuses: maxillary, sphenoid, frontal, and ethmoid. The frontal, maxillary, anterior ethmoid, and middle ethmoid sinuses bilaterally drain to the middle meatuses below the middle conchae. The posterior ethmoid sinuses bilaterally drain to the superior meatuses below the superior concha. The sphenoid sinuses bilaterally drain to the spheno-ethmoid recesses above the superior conchae [4]. The converging paranasal sinus drainage pathways into the nasal tract provide an avenue for the local spread of sinonasal tumors (Figure 1). Additionally, the sphenoid sinus lies inferomedial to the internal carotid artery, optic nerve, pituitary gland, and cavernous sinus while the maxillary sinus is just anterior to the pterygopalatine ganglion as well as the maxillary artery, vein and nerve [4] (Table 1). The important structures which lie in close proximity to the paranasal sinuses may be adversely affected by the growth of sinonasal tumors (Figure 2).

*Corresponding author: Akm A Rahman, Department of Imaging Sciences, University of Rochester Medical Center, USA, E-mail: Akm_Rahman@urmc.rochester.edu

Table 1: Lesion Characteristics.

| Sinonasal Lesion Type	Incidence & Epidemiology	Common Anatomic Locations	General Imaging Findings
Sinonasal Squamous Cell Carcinoma	51.6 % of all sinonasal malignancies [2].	Maxillary sinus, nasal cavity, and ethmoid sinus with local invasion and aggressive bone destruction [1].	Larger tumors exhibit internal signal heterogeneity CT for assessing extent of local invasion and bone destruction T1: Isointense, moderately enhanced on T1+C T2: Hyperintense [1].
Adenocarcinoma	Consists of many histological subtypes. Accounts for 10-20% of sinonasal tumors [1,9].	Intestinal-type (ITAC) can arise from ethmoid sinus, nasal cavity, and maxillary antrum with local invasion to adjacent structures [9].	Occasional areas of calcification reflecting mucin content which alters MRI signal intensity. T1: Gradual contrast enhancement with higher mucin content. T2: Hyperintensity with higher mucin content. Iso-hypointense with lower mucin-content [1].
Adenoid Cystic Carcinoma	Adenocarcinoma subtype. 10% of salivary gland cancers, 5% of sinonasal malignancies [10].	Maxillary sinus and nasal cavity. Possible local extension. Lymph node spread and metastasis to lung, liver, and bone [1,9].	Irregular, heterogeneous mass on MRI T1: Isointense T2: Iso-hyperintense depending on the amount of cellularity [1,10].
SNUC	3-5% of sinonasal cancers [12].	Superior nasal cavity and ethmoid sinus. Location invasion and distant metastases possible [1,12,13].	Ill-defined, non-calcified mass. Central necrosis on CT with contrast. T1: Isointense with heterogeneous contrast enhancement. T2: Iso-hyperintense [1,13].
ENB	0.4 per million incidence, 2-6% of intranasal tumors [14].	Arises from the superior nasal cavity. Local invasion to paranasal sinuses, anterior cranial fossa, cribriform plate and orbit. Metastasis to cervical lymph nodes, lungs, liver, and bone [14].	Possible incidental intracranial lesions. CT for analyzing local invasion and bone involvement. MRI for identifying subtle extent of local invasion, dural seeding, subarachnoid seeding, and metastases. T1: Hypointense T2: Hyperintense [14]
Sinonasal Melanoma	0.5-2% of malignant melanomas and 4% of all head and neck melanomas [15,16].	Nasal cavity, nasal septum, inferior and middle turbinates, lateral nasal wall, and maxillary sinus. Regional and distant metastasis are common [16].	Strong, heterogeneous contrast enhancement on MRI with contrast. T1: Melanin or hemorrhage appear iso-hypointense. Amelanotic appears hypointense. T2: Melanin or hemorrhage may appear iso-hypointense. Amelanotic appears hyperintense [16,17].
Inverted Papilloma	0.4-4% of sinonasal tumors [18].	Locally aggressive, originating from the lateral nasal wall near the middle turbinate or ethmoid recesses, but can extend into the maxillary sinus, ethmoid sinus, and nasopharynx [18].	CT for soft tissue mass and bone remodeling "Convoluted cerebriform" pattern on MRI as alternating high and low signals on T2 and T1 weighted MRI with contrast [18,19].
Antro- choanal Polyp	Most often seen in children with allergies, but also in adults with chronic sinusitis [20].	Arise from the maxillary sinus and pass through the ostea to the choana and nasopharynx [20].	CT: Unilateral hypodense mass from an enlarged opacified maxillary sinus. T1: Iso-hyperintense T2: Iso-hypointense & peripheral enhancement with contrast administration [20].
Mucous Retention Cyst	1.4% to 9.6% of the general population Most common incidental finding in the maxillary sinus [23].	Paranasal sinuses without extension into nasal cavity [23].	T1: Variable to hypointense T2: Hyperintense [23]
Sinonasal Lymphoma	**NHL:** 2nd most frequent sinonasal malignancy. Often in adults >60 and 7-19% of cases show regional lymphadenopathy [1,24].	**NKTL**: Nasal cavity **DLBCL**: Maxillary sinus with intracranial or orbital involvement [25].	**NKTL**: Heterogeneous, intratumoral necrosis, marked contrast enhancement **DLBCL**: Homogenous, mild contrast enhancement [25]. **NHL**: Intratumoral sinus wall remnants on CT if permeative bone invasion across sinus wall is present. Lower ADC in maxillary sinus differentiates from SCC. T1WI: Isointense T2WI: Hyperintense and homogeneous contrast enhancement [1]
Sinonasal Rhabdo-myosarcoma	3–5% of all childhood tumors [26].	Parameningeal (50%), non-parameningeal (25%), and orbital (25%). Parameningeal may arise near skull base structures [26].	CT with contrast: Isodense to hypodense and homogeneously contrast enhancing. T1W1: Isointense to muscle T2W2: Moderately hyperintense to muscle "Botryoid Enhancement Pattern" seen on MRI [27] DWI shows lower mean ADC compared to SCC [28].
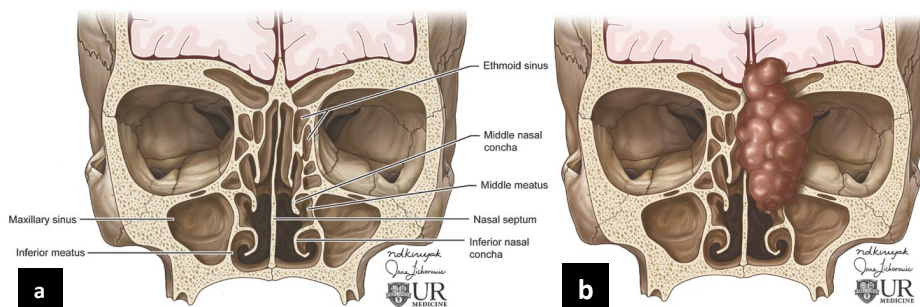
Figure 1: Overview of sinonasal anatomy, coronal illustrations of normal sinonasal tract anatomy (a) and abnormal paranasal sinuses depicting an invasive sinonasal tumor extending from the nasal tract into the skull base, concha, orbit, and maxillary sinus (b).
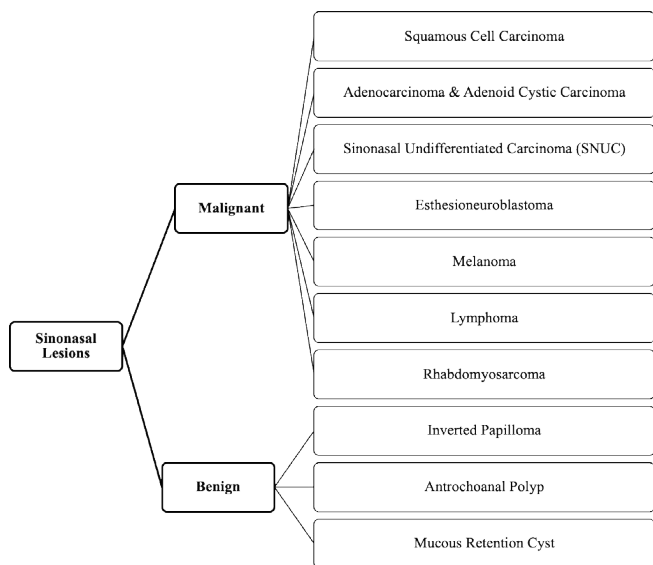
Figure 2: Organization of cases by malignant and benign lesions in the order of presentation.
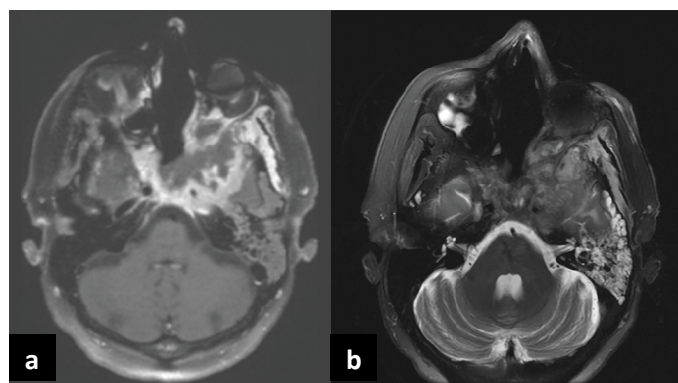

Figure 3: Squamous Cell Carcinoma, Axial T1+C (a) and axial T2 (b) weighted images demonstrate invasive sinonasal squamous cell carcinoma centered in the sphenoid sinuses extending to the adjacent orbit, left middle cranial fossa, and clival region.

Sinonasal Squamous Cell Carcinoma

Sinonasal tumors are more often malignant than benign [1]. Sinonasal squamous cell carcinoma (SCC) is the most common subtype of sinonasal carcinoma accounting for 51.6% of malignant sinonasal tumors [2]. The incidence of sinonasal SCC has been declining from 1973 to 2009, but the overall survival rates have not improved with 20 year overall survival of 30.68% for men and 26.35% for women [5]. SCC most frequently affects the maxillary sinus, nasal cavity, and ethmoid sinus and is characterized by aggressive bone destruction of the adjacent sinus walls as well as local invasion into the opposite sinonasal area, orbital wall, infratemporal fossa, and skull base at more advanced stages. Larger SCC tumors are associated with hypoxic stress leading to internal signal heterogeneity and characteristic regions of intratumoral necrosis. SCC tumors are non-specifically isointense on T1 weighted MRI, faintly hyperintense on T2 weighted MRI, and moderately enhanced on contrast-enhanced T1 weighted MRI. Contrast-enhanced CT may be helpful for evaluating the extent of bone invasion resulting from local tumor extension [1] (Figure 3).

Well known risk factors for squamous cell carcinoma include tobacco smoking and exposure to occupational carcinogens such as softwood and leather dust. Additionally, viral oncogenesis may play a role in sinonasal SCC development and progression [6]. Chowdhury et al. found 16 of 26 (62%) sinonasal tumor biopsy samples were positive for human papilloma virus (HPV) [7]. In another retrospective analysis, Doescher et al. found that only Epstein-Barr virus (EBV) positive sinonasal SCC patients (20/44) developed lymph node or distant metastases further suggesting a role for viral oncogenesis in the progression of sinonasal SCC [8].

Invasive Sinonasal Carcinoma

Many histological subtypes of sinonasal carcinoma including SNUC and adenocarcinoma display locally invasive characteristics involving structures adjacent to the sinonasal tract including the brain, orbit, cranial fossa, nasopharynx, and internal carotid arteries. This can cause diplopia, facial pain, or neurologic signs. Invasive sinonasal adenocarcinoma accounts for 10-20% of sinonasal malignancies [1]. Sinonasal intestinal-type adenocarcinoma (ITAC) exhibit locally invasive characteristics and involve the ethmoid sinus (40%), nasal cavity (25%), and maxillary antrum (20%) [9]. Colonic-type is the most common ITAC and exhibits wide extension into the orbit, pterygopalatine fossa and cranial cavity. Sinonasal ITACs most commonly affect males averaging 50-64 years old and have 1000 times greater prevalence in workers exposed to hardwood dust. Wood-dust related ITACs more commonly arise in the ethmoid sinus while sporadic ITACs more commonly arise in the maxillary antrum [9]. Higher mucin content adenocarcinomas exhibit hyperintensity on T2WI as well as contrast enhancement on T1WI with contrast. Sinonasal ITAC may have a similar imaging presentation to squamous cell carcinoma [1] (Figure 4).

Diagnostic imaging is essential to evaluate the extent of invasion and to predict the histological tumor subtype [1]. CT is more effective for imaging local invasion into bone and identifying intralesional calcifications as well as feeding arteries. Characteristic patterns of bone invasion include extensive bone destruction for high grade malignancies and slow, expansile bone growth for benign lesions or low-grade malignancies [1]. MRI is more effective for greater contrast resolution, differentiating soft tissue regions of a tumor, and detecting perineural spread as well as dural invasion. Malignant tumors are non-specifically hyperintense on T2 weighted imaging and iso-hypo intense on T1 weighted imaging. Higher ADC values (1.35–1.78x10-3 mm2/s) indicate fluid, hypocellularity, cartilage, or mucus which may be more common with benign sinonasal lesions. Lower ADC values (0.87–1.10x10-3 mm/s2) are indicative of hemorrhage, hypercellularity, or abscess which may be implicated in malignant sinonasal tumors [1].
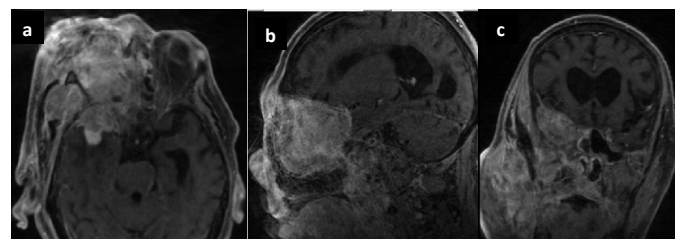

Figure 4: Invasive Sinonasal Carcinoma, Axial (a), sagittal (b), and coronal (c) T1+C images demonstrate invasive sinonasal carcinoma extending to the right orbit, right pterygoid fossa and right middle cranial fossa. AJCC pathologic stage III, grouping pT4bN2b indicative of very advanced local disease. Pathology confirmed SNUC positive for CK7 and pancytokeratin.

Adenoid Cystic Carcinoma

Adenoid cystic carcinoma (ACC) commonly occurs in women in the 5th–6th decade and accounts for 10% of salivary gland tumors and 5% of sinonasal malignancies. Tubular and cribriform are low-grade morphologies, while solid is a higher grade tumor [10]. ACC is slow growing, relentless, and commonly occurs in the maxillary sinus and nasal cavity with possible infiltration into the sphenoid or ethmoid sinuses [1,9]. ACC is characterized by wide expansile or destructive bone defects and perineural or angio invasion. The overall recurrence rate of ACC is 56.2% due to local recurrence, lymph node involvement, and late distant metastases to the lungs, liver and bone [1]. On MRI, ACC appear as an irregular mass of heterogeneous intensity that may be isointense on T1WI and iso-hyperintense on T2WI with variable amounts of cellularity [1,10]. While MRI is more sensitive for ACC detection, CT can be complementary to MRI for characterizing the extent of bone invasion and perineural spread of head and neck ACC [10,11] (Figure 5).

Sinonasal Undifferentiated Carcinoma

Sinonasal undifferentiated carcinoma (SNUC) is a rare tumor with poor overall prognosis which accounts for approximately 3-5% of sinonasal cancers [12]. SNUC is more common in males and often presents as stage IV disease exhibiting aggressive growth, bone destruction, local intracranial and orbital invasion, and distant metastasis [1,12]. SNUC tumors are large (>4 cm) and typically arise in the ethmoid sinus and superior nasal cavity. Local invasion into adjacent structures such as the paranasal sinuses, anterior fossa, orbits, pterygopalatine fossa, parapharyngeal space, and cavernous sinus has been reported [13]. SNUC normally appears as a non-calcified mass with ill-defined margins, bone destruction, variable contrast enhancement, and central necrosis on CT with contrast [13]. On T1WI SNUC appears isointense with heterogeneous enhancement on T1 with contrast. On T2WI SNUC appears iso-hyperintense. SNUC and SCC may present with similar non-specific imaging features [1] (Figure 6).

Olfactory Neuroblastoma (Esthesioneuroblastoma)

Esthesioneuroblastoma (ENB) is an uncommon dumbbell shaped lesion that accounts for 2-6% of intranasal cancers and has an incidence rate of 0.4 cases per million population. ENB arises from the olfactory epithelium in the superior nasal cavity and exhibits aggressive local invasion and metastasis assessed via CT and MRI. ENB can be classified by the conventional tumor, node, metastasis (TNM) system, the Kadish staging system, or the modified TNM Dulguerov staging system. ENB is characterized by slow growth as well as local invasion into the paranasal sinuses, anterior cranial fossa, cribriform plate, and orbit. Metastasis to cervical lymph nodes occurs in > 23% of cases and

Figure 5: Adenoid Cystic Carcinoma, Coronal CT (a), axial T2 MR (b), and coronal T1+C MR (c) images demonstrating an adenoid cystic carcinoma centered in the left maxillary sinus. The hard palate demonstrates post contrast enhancement and osseous erosion.
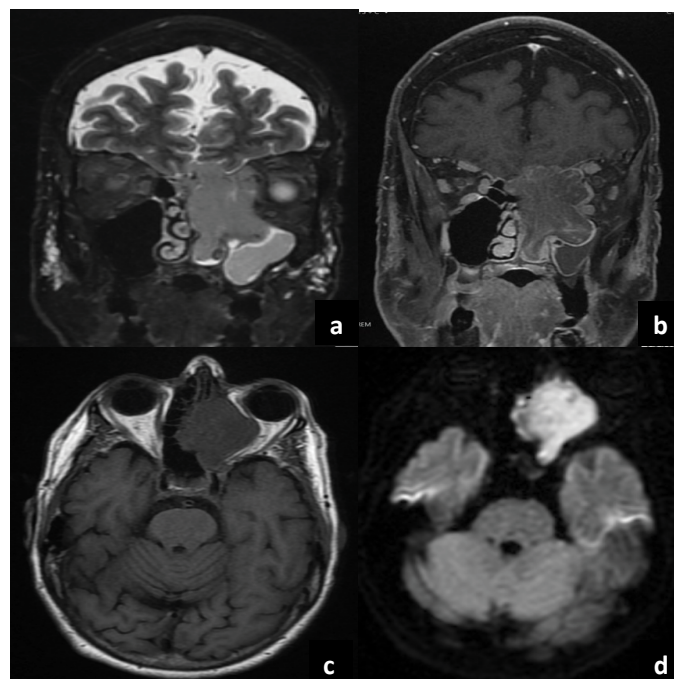

Figure 6: Sinonasal Undifferentiated Carcinoma, Coronal T2 (a), coronal T1+C (b), axial T1 (c), & axial DWI (d) images showing a mass extending from the left maxillary sinus into the orbit and intracranial fossa.
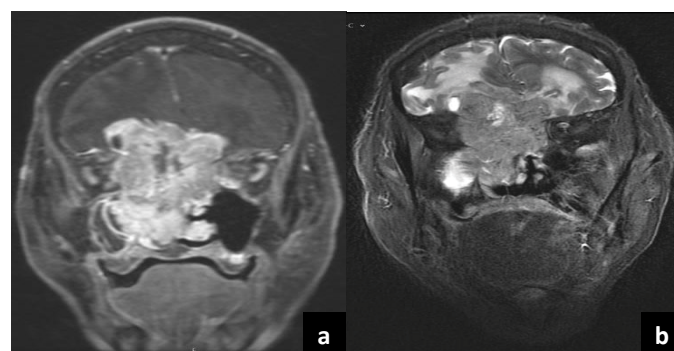

Figure 7: Esthesioneuroblastoma, Coronal T1 + C (a) and coronal T2 (b) images showing an enhancing cystic lesion in the bilateral fossa representing ENB with extension to adjacent orbits and anterior cranial fossa.

metastasis to the neck, lungs, liver, and bone are also common. CT is used to assess for local invasion and bone involvement in ENB while MRI can better define the subtle extent of local invasion and dural or subarachnoid seeding (Figure 7). ENB normally appears hypointense on T1 weighted MRI and hyperintense on T2 weighted MRI. Incidental findings of cystic intracranial lesions are suggestive of ENB [14] (Figure 8).

Sinonasal Melanoma

Sinonasal melanoma is a rare malignant lesion that arises from mucosal melanocytes of the nasal cavity and paranasal sinuses and accounts for 0.3% of all melanomas and less than 5% of all head and neck melanomas [15,16]. Sinonasal melanoma has a 5-year survival of < 35% and sinus melanoma has a worse prognosis than the more common nasal melanoma [16]. The most frequently affected areas are the nasal septum, lateral nasal wall, maxillary antrum, and ethmoid sinuses. In 40-50% of patients, distant metastases via hematogenous spread to the cervical lymph nodes, liver, skin, lung, bone, or brain are
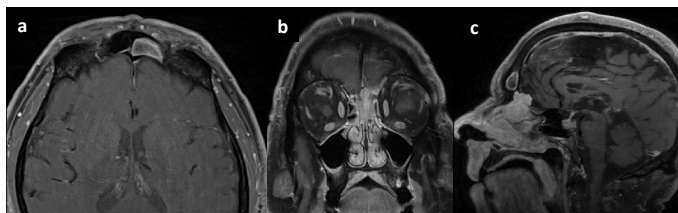
Figure 8: Esthesioneuroblastoma, Axial (a), sagittal (b), and coronal (c) T1 post contrast sequence demonstrates an enhancing cystic lesion (T2W images not shown) centered in the left olfactory fossa, which extends through the cribriform region into anterior middle cranial fossa.
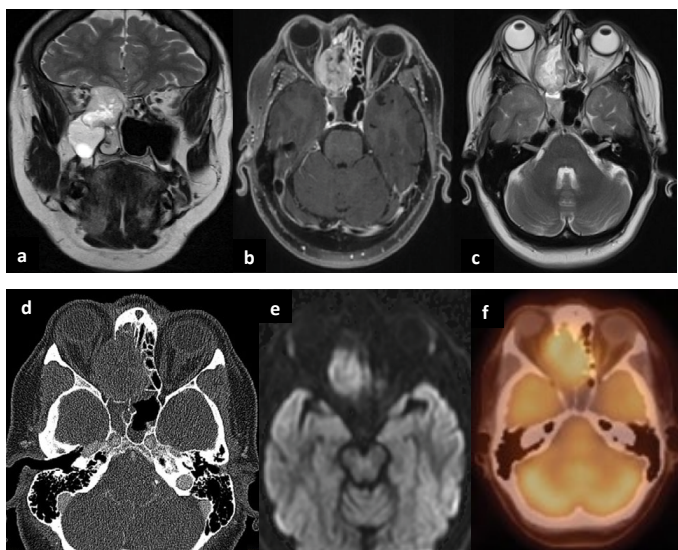

Figure 9: Sinonasal Melanoma, Coronal T2 (a), axial T1 + C (b), axial T2 (c), axial CT bone (d), axial DWI (e), and axial PET (f) images showing an enhancing sinonasal melanoma centered in the right nasal cavity extending into the adjacent right orbit and into the anterior cranial fossa demonstrating diffusion restriction and PET activity.

Figure 10: Axial DWI (a), coronal T2 (b), and coronal T1 + C (c) images showing sinonasal lymphoma centered in the right maxillary sinus extending to the right ethmoid and right inferior orbital margin. Pathology confirmed CD5 and CD10 positive germinal center B cell DLBCL.

commonly found. Deeply invasive local growth can be seen along with recurrence after treatment.16 Similar to other subtypes of sinonasal tumors CT can be used to define the extent of local invasion and bone involvement of the skull base, orbit walls, and carotid canals [1,16].

Sinonasal malignant melanoma may present with melanotic or amelanotic patterns. Generally, melanotic patterns present as iso-hyperintense on T1WI and hypointense on T2WI, while amelanotic patterns present as hypo-isointense on T1WI and hyper-isointense on T2WI relative to the cortex [17,16]. Deviations from this pattern are common, and some studies have indicated internal flow voids suggesting vascular flow networks to be indicative of sinonasal melanoma although this is not a specific diagnostic feature [16] (Figure 9).

Sinonasal Lymphoma

After SCC, NHL is the most frequently observed malignancy in the sinonasal tract, usually in adults over the age of 60, with recent imaging studies showing regional lymphadenopathy as a presenting in 7-19% of cases [1,18]. There are several histological subtypes of sinonasal lymphomas including diffuse large B-cell lymphoma (DLBCL), NK/T cell lymphoma (NKTL), and non-Hodgkin's Lymphoma (NHL). DLBCLs frequently arise from the paranasal sinuses, particularly the maxillary sinus, with intracranial or orbital involvement. NKTLs most often arise from the nasal cavity with Asian and South American populations disproportionately affected.
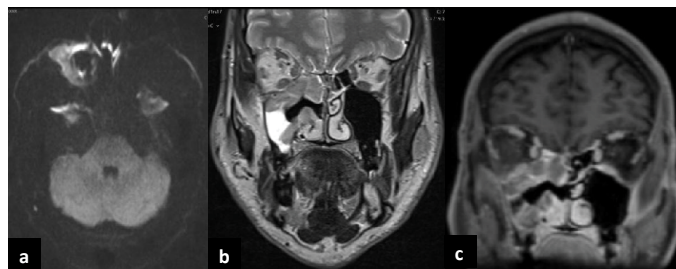
Extra nodal lymphomas are commonly found in the head and neck region. In particular, sinonasal lymphomas demonstrate infiltrative or permeative bone invasion on CT with variable regional bone destruction [1]. MR has shown to be more useful in diagnosis of sinonasal lymphomas, appearing as a mass with soft tissue attenuation [18]. These lesions lack specific clinical signs, leading to late diagnosis, and are monitored, rather than surgically treated.

On imaging, NKTLs are heterogeneous with intratumoral necrosis and marked enhancement, whereas DLBCL is homogenous with mild enhancement [19]. On CT, NHLs that involve permeative bone invasion across the sinus wall demonstrate intra-tumoral sinus wall remnants. NHLs appear isointense on T1 weighted MRI and hyperintense on T2 weighted MRI, and are homogeneously enhanced. NHLs in the maxillary sinus typically have a lower ADC, which is used to differentiate NHLs from SCC [1] (Figure 10).

Sinonasal Rhabdomyosarcoma

Rhabdomyosarcoma (RMS) is a common soft tissue tumor that constitutes 3–5% of all childhood tumors. RMS can arise from primitive mesenchymal cells anywhere in the body and 40% of childhood RMS occur in the head and neck region. There are three recognized primary locations for head and neck RMS including parameningeal (50%), non-parameningeal (25%), and orbital (25%). Parameningeal RMS typically have the lowest 5-year overall survival followed by non-parameningeal then orbital locations. The deeper parameningeal location may conceal the tumor until it presents symptomatically at a later stage. Additionally, parameningeal RMS can arise adjacent to vital nearby skull base structures including the internal carotid arteries, cranial nerves, and jugular veins resulting in symptomatic cranial nerve palsy, intracranial extension, and skull base erosion [20].

RMS can be classified into three main histological subgroups including embryonal, alveolar, and pleomorphic. The embryonal RMS subtype accounts for 70% of cases and typically presents in younger age individuals with a better prognosis. Alveolar RMS accounts for 15% of head and neck RMS and presents in older children with a worse prognosis. The overall clinical presentation depends on the primary tumor location, presence of metastasis, and the histological subtype of the RMS tumor [20].

Imaging is essential for the diagnosis of RMS and assessment of chemotherapy response, recurrence, and distant metastases [20]. Head and neck RMS present with bone destruction and extension into adjacent structures. On CT, head and neck RMS present as isodense to hypodense and homogeneously contrast enhancing on CT with contrast. On MRI, head and neck RMS appear isointense to muscle on T1WI and moderately hyperintense to muscle on T2WI. RMS may also

demonstrate a botryoid enhancement pattern on MRI [21]. On T1-weighted MRI with intravenous contrast, head and neck RMS appear with moderate homogenous enhancement and variable enhancement patterns. Diffusion weighted imaging (DWI) may better allow for identification of RMS in comparison to SCC, as RMS has been shown to have lower mean ADC [22] (Figure 11).

Inverted Papilloma

Inverted papilloma (IP) represent 0.4-4% of sinonasal tumors, originating from the lateral nasal wall near the middle turbinate or ethmoid recesses [23]. These are locally aggressive, benign neoplasms, though large IPs can extend into the maxillary sinus, ethmoid sinus, and nasopharynx. IPs often have high recurrence after surgery, with a recurrence rate of 2-15% [23]. Initial evaluation for IPs involves CT for soft tissue mass and bone remodeling, rather than bone destruction. MRI + contrast helps differentiate IPs from inflammatory antrochoanal polyps, which display peripheral contrast enhancement. IPs appear iso- to hypointense on T1 weighted MRI and hyperintense to muscle on T2 weighted MRI. A "convoluted cerebriform" pattern on MRI is visualized in up to 80% of IP patients as alternating high and low signals on T2 and T1 weighted MRI with contrast. Though this pattern may also be seen on MRI with malignant neoplasms, it has been shown in retrospective studies to be a reliable MR pattern for IPs [23,24] (Figure 12).

Antrochoanal Polyp

Antrochoanal Polyps (AP) are rare, benign mucosal lesions with solid and cystic components. APs typically arise from the maxillary sinus and pass through the ostia 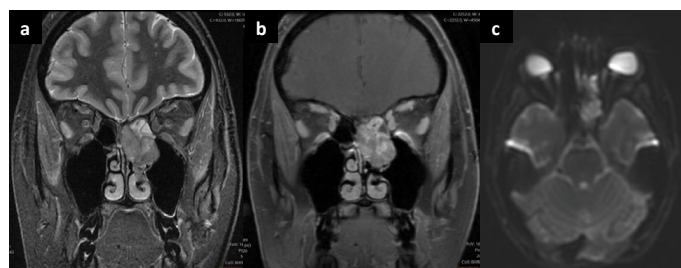to the choana and nasopharynx. These polyps are indicative of chronic inflammation, most often seen in children with allergies, but also in adults with chronic sinusitis [25]. Similar to IPs, APs do not involve bone destruction. The only known risk factor for APs are anatomical abnormalities, the most common being nasal septal deviation, inferior turbinate hypertrophy, and concha bullosa. Both the solid and cystic components of polyps are removed through functional endoscopic sinus surgery (FESS) to reduce complication and recurrence. Despite the high success rate, APs treated with FESS can still have up to a 15% recurrence rate [25-27]. On CT, APs appear as a unilateral hypodense mass from an enlarged opacified maxillary sinus. APs are iso-hyperintense on T1 weighted MRI and iso-hypointense on T2 weighted MRI, and demonstrate peripheral enhancement with contrast administration [25] (Figure 13).

Mucous Retention Cyst

Mucus retention cysts (MRCs) are benign lesions in the paranasal sinuses representing obstructed submucosal mucinous glands. MRCs present similarly to sinonasal polyps, but without extension into the nasal cavity. Though MRCs are often asymptomatic and exhibit spontaneous regression, they can present with headache, periorbital pain, and nasal obstruction, necessitating endoscopic surgical resection (Figure 14). These cysts are reported to occur in 1.4% to 9.6% of the general population and are the most common incidental finding in the maxillary sinus [28]. In a retrospective analysis of 510 paranasal sinus CT scans, MRCs were found in 29.4% of cases. MRCs are variable to hypointense on T1 weighted MRI and hyperintense on T2 weighted MRI [28] (Figure 15).

Figure 11: Coronal T2 (a), coronal T1 + C (b), and axial DWI (c) showing sinonasal rhabdomyosarcoma centered in the left ethmoid demonstrating enhancement and diffusion restriction.
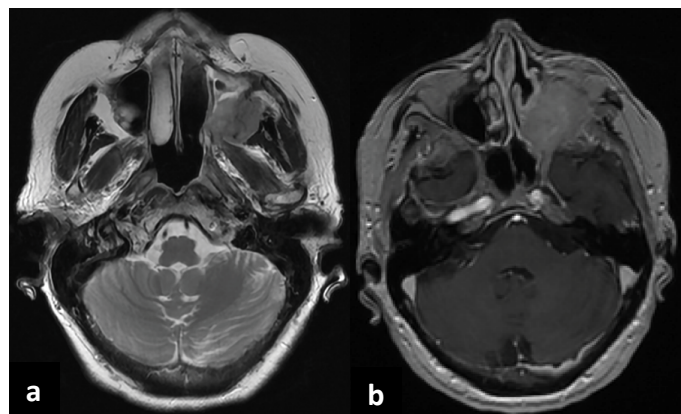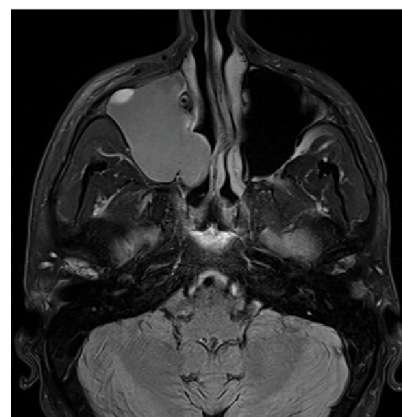

Figure 13: Antrochoanal Polyp, Axial T2 weighted image demonstrates an antrochoanal polyp centered in the right maxillary sinus extending through the osteomeatal unit into the nasal cavity.

Figure 12: Inverted Papilloma, Axial T2 (a) and T1+C (b) images demonstrate an enhancing soft tissue mass of the left maxillary sinus representing an inverted papilloma.
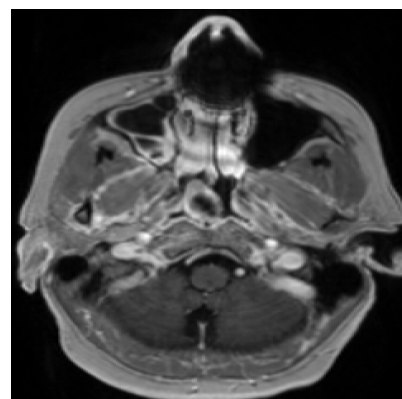

Figure 14: Mucous Retention Cyst, A mucous retention cyst in the right sphenoid sinus.

Figure 15: Mucous Retention Cyst, Axial (a), sagittal (b), and coronal (c) CT head images demonstrate a retention cyst in the left sphenoid sinus.

Conclusion

General clinical features of sinonasal tumors may include headache, epistaxis, and diplopia, while more specific features include altered phonation, facial pain, palpable masses, neurologic signs, and anosmia. The local spread of sinonasal tumors beyond the sinonasal tract may impact adjacent structures including the internal carotid artery, skull base, and orbit. Diagnostic imaging is essential to determine the extent of local tumor invasion and to identify lymph node involvement as well as distant metastasis to organs such as the lungs, liver, kidney, bone, and brain. Imaging features alongside histological data and the presence of metastatic disease contribute to the staging, prognosis, and treatment planning for sinonasal tumors.

References

1. Kawaguchi M, Kato H, Tomita H (2017) Imaging Characteristics of Malignant Sinonasal Tumors. J Clin Med 6: 116.

2. Turner JH, Reh DD (2011) Incidence and survival in patients with sinonasal cancer: A historical analysis of population-based data. Head Neck 34: 877-885.

3. Razek AA, Sieza S, Maha B (2009) Assessment of nasal and paranasal sinus masses by diffusion-weighted MR imaging. J Neuroradiol 36: 206-211.

4. Cappello ZJ, Minutello K, Dublin AB (2023) Anatomy, Head and Neck, Nose Paranasal Sinuses. In: StatPearls.

5. Sanghvi S, Khan MN, Patel NR (2014) Epidemiology of sinonasal squamous cell carcinoma: a comprehensive analysis of 4994 patients. Laryngoscope 124: 76-83.

6. Elgart K, Faden DL (2020) Sinonasal Squamous Cell Carcinoma: Etiology, Pathogenesis, and the Role of Human Papilloma Virus. Curr Otorhinolaryngol Rep 8: 111-119.

7. Chowdhury N, Alvi S, Kimura K (2017) Outcomes of HPV-related nasal squamous cell carcinoma. Laryngoscope 127: 1600-1603.

8. Doescher J, Piontek G, Wirth M (2015) Epstein-Barr virus infection is strictly associated with the metastatic spread of sinonasal squamous-cell carcinomas. Oral Oncol 51: 929-934.

9. Leivo I (2016) Sinonasal Adenocarcinoma: Update on Classification, Immunophenotype and Molecular Features. Head and Neck Pathol 10: 68–74.

10. Sepúlveda I, Platin E, Delgado C (2015) Sinonasal Adenoid Cystic Carcinoma with Intracranial Invasion and Perineural Spread: A Case Report and Review of the Literature. J Clin Imaging Sci 5: 57.

11. Uraizee I, Cipriani NA, Ginat DT (2018) Adenoid Cystic Carcinoma of the Oral Cavity: Radiology-Pathology Correlation. Head Neck Pathol 12: 562-566.

12. Xu CC, Dziegielewski PT, McGaw WT (2013) Sinonasal undifferentiated carcinoma (SNUC): the Alberta experience and literature review. J Otolaryngol Head Neck Surg 42: 2.

13. Phillips CD, Futterer SF, Lipper MH (1997) Sinonasal undifferentiated carcinoma: CT and MR imaging of an uncommon neoplasm of the nasal cavity. Radiology 202: 477-480.

14. Dublin AB, Bobinski M (2016) Imaging Characteristics of Olfactory Neuroblastoma (Esthesioneuroblastoma). J Neurol Surg B Skull Base 77: 1-5.

15. Gore MR, Zanation AM (2012) Survival in Sinonasal Melanoma: A Meta-analysis. J Neurol Surg B Skull Base 73: 157-162.

16. Wong VK, Lubner MG, Menias CO (2017) Clinical and Imaging Features of Noncutaneous Melanoma. AJR Am J Roentgenol 208: 942-959.

17. Escott EJ (2001) A variety of appearances of malignant melanoma in the head: a review. Radiographics 21: 625-639.

18. Bitner BF, Htun NN, Wang BY (2022) Sinonasal lymphoma: A primer for otolaryngologists. Laryngoscope Investig Otolaryngol 7: 1712-1724.

19. Chen Y, Wang X, Li L (2020) Correction to: Differential diagnosis of sinonasal extranodal NK/T cell lymphoma and diffuse large B cell lymphoma on MRI. Neuroradiology 62: 1201.

20. Freling NJ, Merks JH, Saeed P (2010) Imaging findings in craniofacial childhood rhabdomyosarcoma. Pediatr Radiol 40: 1723-1738.

21. Liu JH, Qi M, Huang WH (2023) The magnetic resonance characteristics of sinonasal rhabdomyosarcoma in adults: analysis of 27 cases and comparison with pathological subtypes. BMC Med Imaging 23: 98.

22. Wang X, Song L, Chong V, Wang Y, Li J, et al. (2017) Multiparametric MRI findings of sinonasal rhabdomyosarcoma in adults with comparison to carcinoma. J Magn Reson Imaging 45: 998-1004.

23. Chawla A, Shenoy J, Chokkappan K (2016) Imaging Features of Sinonasal Inverted Papilloma: A Pictorial Review. Current Problems in Diagnostic Radiology 45: 347-353.

24. Eid M, Eissa L (2020) Imaging of sino-nasal inverted papilloma: How can we emphasize the usefulness of the "striated pattern" sign? Egypt J Radiol Nucl Med 51: 29.

25. Chagarlamudi K, O'Brien WT, Towbin RB (2019) Antrochoanal polyp. Appl Radiol 48: 38-40.

26. Pagella F, Emanuelli E, Pusateri A (2018) Clinical features and management of antrochoanal polyps in children: Cues from a clinical series of 58 patients. Int J Pediatr Otorhinolaryngol 114: 87-91.

27. Lee DH, Yoon TM, Lee JK (2016) Difference of antrochoanal polyp between children and adults. Int J Pediatr Otorhinolaryngol 84: 143-146.

28. Bal M, Berkiten G, Uyanık E (2014) Mucous retention cysts of the paranasal sinuses. Hippokratia 18: 379.